ACS OMEGA

http://pubs.acs.org/journal/acsodf

Article

Growth of Pentacene Crystals by Naphthalene Flux Method

Xiaoran Yang, Mingzhe Li, Akira Maeno, Takashi Yanase, Seiya Yokokura, Taro Nagahama, and Toshihiro Shimada*

Cite This: *ACS Omega* 2022, 7, 28618−28623

Read Online

ACCESS | Metrics & More | Article Recommendations | Supporting Information

ABSTRACT: We report the crystal growth of pentacene from a solution of naphthalene. The solubility of pentacene in naphthalene was evaluated by optical absorption at elevated temperature. The crystal growth was performed in an H-shaped sealed glass tube or metal vessels sealed with ultrahigh-vacuum compatible flanges placed in heated two-zone aluminum blocks. The obtained crystals had a single-crystal-like appearance and flat surface. They were made of aligned microtwins of the "bulk type" (interlayer spacing 14.5 Å) polymorph.

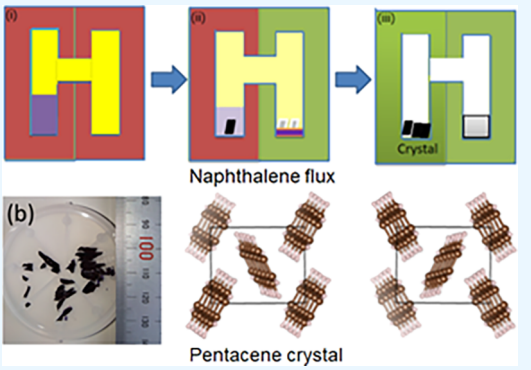

INTRODUCTION

Organic semiconductors are recently gathering much attention for their application in flexible, light-weight, and printable electronic circuits.[1−9] It is necessary to design and synthesize molecules with a high performance for such applications, but there are still some "missing links" connecting molecular structures and the physical properties of the organic semiconductor materials. They include carrier mobilities, exciton binding energies, lifetimes, etc. It is highly desirable to make crystals of organic semiconductors and experimentally study their crystal structures and various physical properties in order to find a way to connect the molecular structures and the important physical properties as semiconductors, along with various applications summarized in recent reviews.[10−13]

Pentacene ($C_{14}H_{22}$) is an important organic semiconductor from the early days of research.[14−28] Pentacene stands out for its relatively high field effect mobility. Its hole mobility is as high as 35 $cm^2/(V{\cdot}s)$ in one report,[22] which exceeds amorphous silicon.

In this study, we focused on a new method called the "naphthalene flux method"[29,30] to grow the pentacene crystals. This method uses a solid aromatic molecule (naphthalene; melting point, 80.2 °C) as the solvent, or flux, of the pentacene. It is well known that pentacene decomposes above its melting point; thus, the melt growth technique cannot be applied. The physical vapor transport (PVT) technique has mainly been used for the single crystal growth of molecules including pentacene for the device applications.[31−34] The solubility of pentacene in ordinary organic solvents is poor.[35,36] A 1,2,4-trichlorobenzene solution at 140 °C was used to grow pentacene thin film crystals to make transistors,[37,38] but the sizes of the crystals were quite inferior to that obtained by the PVT.

We experimentally searched for a solvent of pentacene and found that pentacene can be dissolved in a naphthalene solution. The growth of crystal in solution will be easier to control, and the size of the crystals obtained by "naphthalene flux method" was comparable to or larger than that of the crystals obtained by the PVT method.

EXPERIMENTAL SECTION

Solubility Measurement. We first determined the temperature that is suitable for its crystal growth by measuring the solubility of pentacene in naphthalene. We measured the optical absorption of heated solutions of pentacene in naphthalene with excess amounts of pentacene. Since the optical density of a pentacene solution is high, the thickness of the solution must be thin. We used a glass capillary (2.4 mm inner diameter) to hold the solution. This requires handling of a very tiny amount of pentacene. Therefore, the typical procedure was as follows.

About 1 mg of pentacene was placed in a test tube with 100 μL of chlorobenzene, which was pumped to 10 Pa and sealed by melting the glass tube. The test tube was then heated to 120 °C to dissolve the pentacene. A clear purple solution was

Received: June 7, 2022
Accepted: July 22, 2022
Published: August 2, 2022

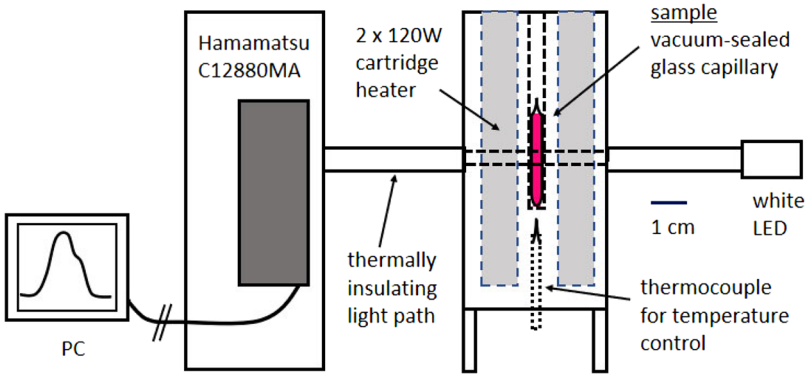

Figure 1. Solubility measurement device.

obtained. The test tube was next opened while hot; 20 μL of the solution was transferred to the capillary by a micropipette; and the chlorobenzene was evaporated by heating it at 140 °C with pumping. About 400 mg of naphthalene was then added to the capillary, and the capillary was vacuum sealed.

We placed the sealed capillary in a temperature-controlled aluminum block, which had light able to pass through both sides (Figure 1). By heating the aluminum block, the naphthalene first melted at ~80 °C; then, the pentacene started to dissolve into the naphthalene. The optical absorption of the solution was measured by a white LED light source and microspectrometer (Hamamatsu C12880MA; with Color Compass software). We recorded the absorption spectra every 10 °C. The concentration was calculated based on the Lambert−Beer formula:

$$\log_{10}(I_0/I) = \varepsilon bc \quad (1)$$

where I_0 and I are the intensities (or power) of the incident light and the transmitted light, respectively. ε is the molar absorption coefficient, b is the light path (inner diameter of the capillary), and c is the concentration. I_0 was measured by setting a capillary containing only naphthalene as a blank. Because ε is not known, we used the concentration at which all the pentacene was dissolved to calibrate the concentration c (see next section).

Crystal Growth. Since the materials are air sensitive at elevated temperatures[35,36] and naphthalene is highly volatile,[39,40] the growth process was performed in a vacuum-sealed H-shaped glass tube. The heater used in this experiment can be separately controlled on both sides. The method is schematically illustrated in Figure 2a. (i) Pentacene is completely dissolved into naphthalene by elevating the temperature of both sides. The right side was then set at a slightly lower temperature, and both sides were very slowly cooled. The pentacene crystal grew in the left side. The right side was cooled first before the naphthalene on the left side had solidified in order to collect the naphthalene on the right side by vapor transport (ii). At the end, the left side contained pentacene crystal and the naphthalene was completely collected on the right side (iii). A typical temperature profile is shown in Figure 2b. Some images about the growth experiment can be found in the Supporting Information (Figures S1 and S2).

We also scaled up the crystal growth system using an ultrahigh vacuum compatible apparatus sealed with ConFlat flanges and metal bellow valves.

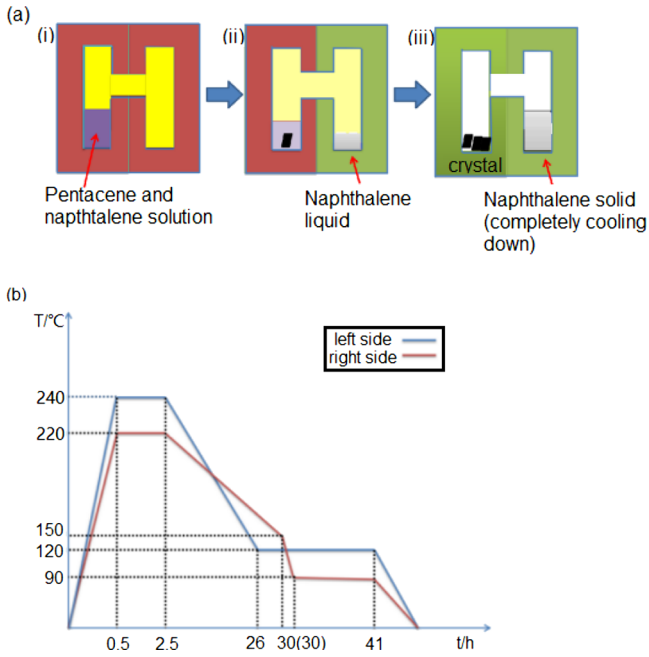

Figure 2. Crystal growth scheme. (a) Schematics of the naphthalene flux method. (b) Temperature (T)−time(t) profiles of the left and right sides.

Characterization. The surface morphology of the pentacene crystal was observed by a laser microscope (Keyence KN-7200). Polarization optical microscopy (Olympus BX51) was used to evaluate the crystal orientation of the pentacene crystal. The θ−2θ (Rigaku Miniflex 600) and pole figure (Rigaku SmartLab) X-ray diffraction (XRD) were used to evaluate the crystallinity and the crystal structure.

RESULTS AND DISCUSSION

The solubility of pentacene in naphthalene at RT is low, while the solubility will gradually increase as the temperature increases. Figure 3a shows the sample used for the solubility measurement, and Figure 3b is the obtained absorbance curve.

Figure 4 shows the optical absorbance at 528 nm of two samples containing 0.20 and 0.15 wt % of pentacene in naphthalene as a function of the temperature. As noted, the two curves agree at the lower temperatures, but the curve for the lower pentacene content becomes constant at 230 °C. This result can be explained as follows.

The concentration of the pentacene in the solution should be approximately the same at the beginning because all of the

https://doi.org/10.1021/acsomega.2c03551
ACS Omega 2022, 7, 28618−28623

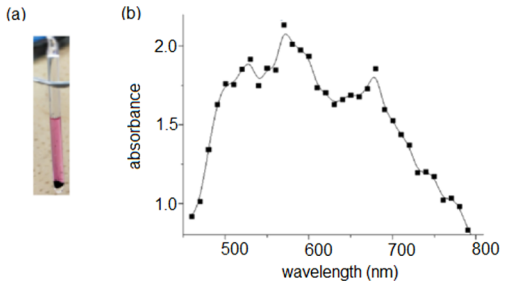

Figure 3. (a) Solubility measurement sample (pentacene−naphthalene at 90 °C). (b) Absorbance spectrum of pentacene dissolved in naphthalene.

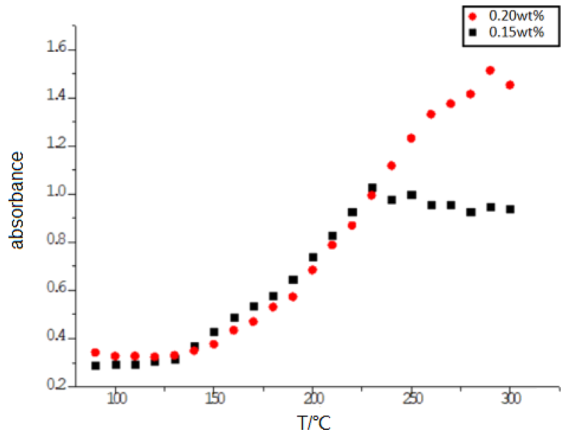

Figure 4. Solubility measurement curves of pentacene in naphthalene. (a) and (b) contain 0.20 and 0.15 wt % pentacene in naphthalene, respectively.

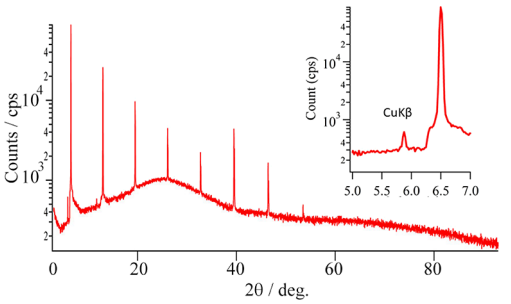

Figure 6. Out-of-plane X-ray diffraction of a pentacene plate-like crystal.

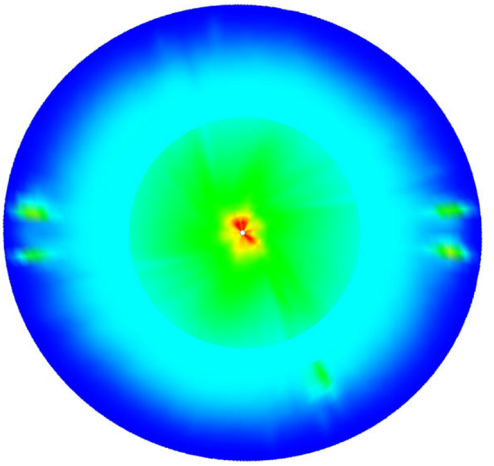

Figure 7. Pole figure of pentacene crystal (2θ = 17.7°).

soluble pentacene is dissolved in equilibrium with the pentacene solid. The solubility then increases with the temperature, and the curve becomes a straight line after the pentacene is completely dissolved. The absorbance value of the straight line corresponds to εbc in eq 1. We can calculate c from the pentacene:naphthalene ratio charged in the capillary, and b is from the diameter of the capillary. If we assume that the molar absorption coefficient of pentacene in naphthalene is a constant, we can evaluate ε from the data shown in Figure 5, which was ∼1.1 × 10^3 L mol^{-1} cm^{-1}. The error remains in the ε value because it is difficult to estimate the light path in a capillary with accuracy.

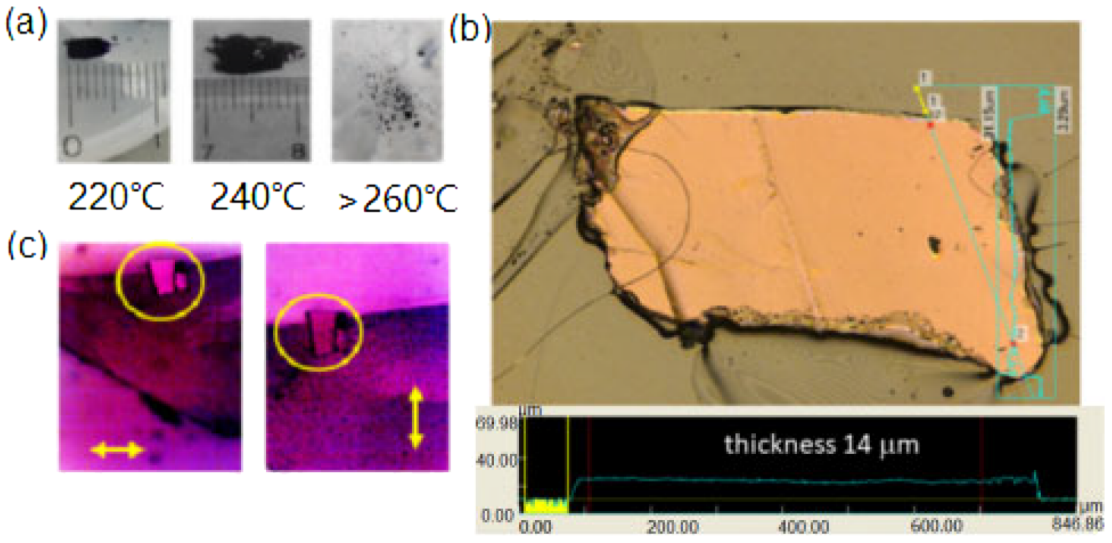

Figure 5. (a) Obtained pentacene crystals at different growth temperatures by the naphthalene flux method. (b) Laser microscope image of a pentacene crystal. (c) Polarization microscope images of a pentacene crystal. The brightness of the crystal changed (see circle) when the dial was rotated 90°.

https://doi.org/10.1021/acsomega.2c03551
ACS Omega 2022, 7, 28618−28623

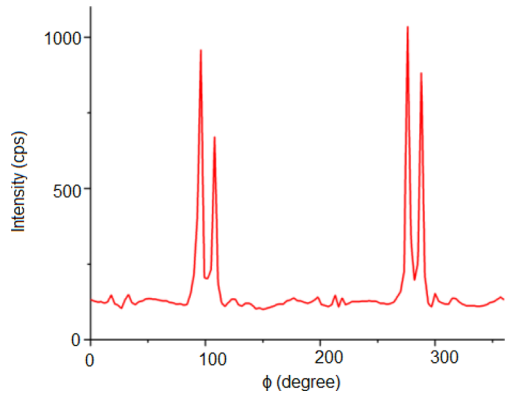

Figure 8. Φ (β) scan of pole figure spot (2θ = 17.7°, α = 16°).

The obtained solubility and temperature data were used as the basis to determine the condition for crystal growth. We used a 0.15 wt % pentacene mixture with naphthalene, and the temperature profile is shown in Figure 2b. The periods and temperatures in the profile were determined on a trial-and-error-basis. Some of the pentacene crystals at different maximum temperatures are shown in Figure 5a. We found that pentacene crystals can be obtained at the highest temperatures of 220−240 °C, and the largest crystal (about 1.1 cm) was obtained at 240 °C. When the highest temperature is above 260 °C, the results were not stable and most of the crystals were a powder. We picked the crystal with well-defined faces and removed any visible impurities under the microscope and then cleaned the surface with acetone for subsequent measurements. Figure 5b shows a laser microscope image of a pentacene crystal in order to measure the thickness and evaluate the flatness of the surface. The thickness of crystal was about 14 μm; it is a plate-like crystal. A piece of the pentacene crystal was characterized by a polarization microscope (Figure 5c). We can see the change in the contrast by rotating the sample, which is caused by the optical anisotropy of the pentacene crystal.

The sample was characterized by X-ray diffraction to determine the crystal structure. Figure 6a shows the out-of-plane (θ−2θ) scan X-ray diffraction. It shows periodic peaks corresponding to the layered stacking of the herringbone lattice of pentacene. There are more than 10 reported structures of pentacene, which are basically classified into three groups,[41−46] *i.e.*, the "bulk type" (layer spacing d = 14.5 Å; high temperature form), single crystal type (d = 14.5 Å; obtained by PVT), and "thin film type" (d = 15.5 Å; obtained by thin film deposition). The differences in these structures are rather slight, but the electronic band structure is very dependent on the polytype.[47] We can rule out the possibility of the "thin film phase" because the (0 0 1) diffraction appears below 2θ = 6.0°. From the out-of-plane scan, it is suggested that the "bulk type" is formed. However, the large single crystals can be somewhat warped during the handling, and the accuracy of interlayer spacing (d) from this XRD is not conclusive. The three-dimensional lattice parameters must be evaluated to confirm the crystal structure.

We measured a pole figure of the pentacene plate crystal by 5-axis XRD equipment (Figure 7). 2θ was set to 17.7°, which corresponds to the (1 1 1) diffraction for the single crystal type and (1 0−3) diffraction for the bulk type. The result is shown in Figure 8. Four spots appeared. It shows that the plate-like pentacene crystal is made of twins. To analyze the orientations of the twins, we calculated the diffraction peaks of each polytype of pentacene near 2θ = 17.7°.

By calculating the reciprocal lattice of each unit lattice, we have identified the spots in the pole figure, which appeared 11−18° off from the surface normal (α), that is, the (1 0−3) diffraction of the "bulk type" pentacene (α = 16°). The (1 1 1) diffraction of the "single crystal type" should appear at α = 69°, which is distinctly different from the result.

As for the twin orientation, each {1 0−3} diffraction is separated into two spots. This means that the a^* and/or c^* axes are separated in the reciprocal space. Because the a−b plane of the layered structure should be common to explain the flatness of the crystal surface, the c^* axis is also common. It follows that the b axis in the real space has different directions in the twin. Assuming that the a axis is common, the Φ (β) scan shown in Figure 8, which shows a 12° separation of the two-fold symmetric peaks, can be reasonably explained. The model structure of the twins in the real space is Figure 9, which was drawn using a software VESTA[48] using the atomic coordinate in ref 40. The model structure of the twins in the real space is shown in Figure 9. The competition among weak interactions, anisotropic van der Waals force and the coincident epitaxy, determines the twinning in pentacene on aligned polymer substrates.[49] We consider that this concept can also be applied to the present case because the coincident epitaxial relation is maintained if the twinned layer is formed on a pentacene surface. As for the size of each twin crystal, we could not resolve the distribution by geometrically scanning the XRD spot, which means that it was smaller than the X-ray spot (0.5 mm) of the measurement. The detail of the XRD data analysis is found in the Supporting Information (Tables S1−S4, Figure S3).

Finally, we examined the possibility of scaling up the growth apparatus. Although H-shaped glass tubes are good for a laboratory scale, it is too time-consuming for the production.

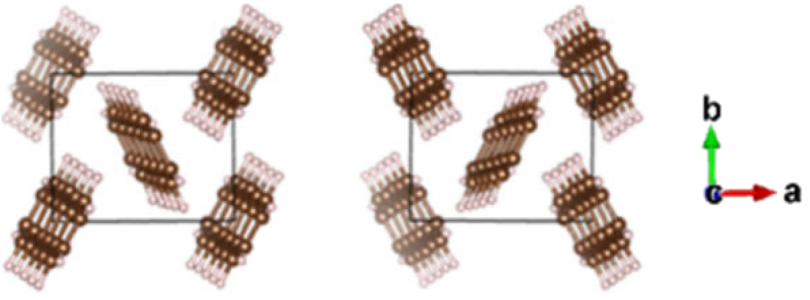

Figure 9. Model of the twin structure.

https://doi.org/10.1021/acsomega.2c03551
ACS Omega 2022, 7, 28618−28623

Figure 10. (a) Scaling up of the growth apparatus. (b) Obtained pentacene crystals.

We have built an ultrahigh-vacuum compatible stainless steel two-room vessel as shown in Figure 10a. By using a two zone furnace and a similar temperature profile as described above, we succeeded in the growth of pentacene crystals shown in Figure 10b.

CONCLUSIONS

In this experiment, we determined the suitable temperature and concentration for pentacene crystal growth from a naphthalene flux solution. The relatively high solubility of pentacene in naphthalene (0.15 wt % at 230 °C and more in elevated temperatures) provides the possibility for pentacene inkjet printing application. Through trial and error, we successfully established the growth parameter and obtained plate-like crystals of pentacene with almost 1 cm sizes. We analyzed the crystal structure by X-ray diffraction and found that "bulk type" (interlayer spacing 14.5 Å) polymorph crystals were formed. The crystals were made of aligned microtwins.

ASSOCIATED CONTENT

Supporting Information

The Supporting Information is available free of charge at https://pubs.acs.org/doi/10.1021/acsomega.2c03551.

Images during experiments and analysis of X-ray diffraction index of pentacene polymorphs (PDF)

AUTHOR INFORMATION

Corresponding Author

Toshihiro Shimada − *Division of Applied Chemistry, Hokkaido University, Sapporo 060-8628, Japan;* orcid.org/0000-0001-5122-1063; Email: shimadat@eng.hokudai.ac.jp

Authors

Xiaoran Yang − *Division of Applied Chemistry, Hokkaido University, Sapporo 060-8628, Japan*

Mingzhe Li − *Division of Applied Chemistry, Hokkaido University, Sapporo 060-8628, Japan*

Akira Maeno − *Division of Applied Chemistry, Hokkaido University, Sapporo 060-8628, Japan*

Takashi Yanase − *Division of Applied Chemistry, Hokkaido University, Sapporo 060-8628, Japan;* Present Address: Department of Chemistry, Toho University, Funabashi; orcid.org/0000-0002-5625-9308

Seiya Yokokura − *Division of Applied Chemistry, Hokkaido University, Sapporo 060-8628, Japan*

Taro Nagahama − *Division of Applied Chemistry, Hokkaido University, Sapporo 060-8628, Japan*

Complete contact information is available at: https://pubs.acs.org/10.1021/acsomega.2c03551

Notes

The authors declare no competing financial interest.

ACKNOWLEDGMENTS

Instrumental analyses were supported by the Nanotechnology platform at Hokkaido University by the METI, Japan. This research was partly supported by JST SPRING (JPMJSP2119).

REFERENCES

(1) Forrest, S. R. The Path to Ubiquitous and Low-Cost Organic Electronic Appliacnces on Plastic. *Nature* **2004**, *428*, 911−918.

(2) Kaltenbrunner, M.; Sekitani, T.; Reeder, J.; Yokota, T.; Kuribara, K.; Tokuhara, T.; Drack, M.; Schwödiauer, R.; Graz, I.; Bauer-Gogonea, S.; Bauer, S.; Someya, T. An Ultra-Lightweight Design for Imperceptible Plastic Electronics. *Nature* **2013**, *499*, 459−463.

(3) Garnier, F.; Hajlaoui, R.; Yassar, A.; Srivastava, P. All-Polymer Field-Effect Transistor Realized by Printing Techniques. *Science* **1994**, *265*, 1684−1686.

(4) Beaujuge, P. M.; Fréchet, J. M. J. Molecular design and ordering effects in π-functional materials for transistor and solar cell applications. *J. Am. Chem. Soc.* **2011**, *133*, 20009−20029.

(5) Minemawari, H.; Yamada, T.; Matsui, H.; Tsutsumi, J.; Haas, S.; Chiba, R.; Kumai, R.; Hasegawa, T. Inkjet Printing of Single-Crystal Films. *Nature* **2011**, *475*, 364−367.

(6) Shi, Y.; Jiang, L.; Liu, J.; Tu, Z.; Hu, Y.; Wu, Q.; Yi, Y.; Gann, E.; McNeill, C. R.; Li, H.; Hu, W.; Zhu, D.; Sirringhaus, H. Bottom-up Growth of n-type Monolayer Molecular Crystals on Polymeric Substrate for Optoelectronic Device Applications. *Nat. Commun.* **2018**, *9*, 2933.3.

(7) Le, D. C.; Nguyen, D. D.; Lloyd, S.; Suzuki, T. K.; Murata, H. Degradation of fluorescent organic light emitting diodes caused by quenching of singlet and triplet excitons. *J. Mater. Chem. C* **2020**, *8*, 14873−14879.

(8) Zhang, Q. Shooting flexible electronics. *Front. Phys.* **2021**, *16*, 13602.

(9) Uoyama, H.; Goushi, K.; Shizu, K.; Nomura, H.; Adachi, C. Highly efficient organic light-emitting diodes from delayed fluorescence. *Nature* **2012**, *492*, 234−238.

(10) Matsui, H.; Takeda, Y.; Tokito, S. Flexible and printed organic transistors: From materials to integrated circuits. *Org. Electron.* **2019**, *75*, No. 105432.

(11) Jiang, H.; Wenping, H. The Emergence of Organic Single-Crystal Electronics. *Angew. Chem., Int. Ed.* **2020**, *59*, 1408−1428.

(12) Chen, W.; Yu, F.; Xu, Q.; Zhou, G.; Zhang, Q. Recent Progress in High Linearly Fused Polycyclic Conjugated Hydrocarbons (PCHs, n > 6) with Well-Defined Structures. *Adv. Sci.* **2022**, *7*, 1903766.

(13) Zhang, Z.; Zhang, Q. Recent progress in well-defined higher azaacenes (n ≥ 6): synthesis, molecular packing, and applications. *Mater. Chem. Front.* **2020**, *4*, 3419−3432.

(14) Minakata, T.; Nagoya, I.; Ozaki, M. Highly Ordered and Conducting Thin Film of Pentacene Doped with Iodine Vapor. *J. Appl. Phys.* **1991**, *69*, 7354.

(15) Ruiz, R.; Choudhary, D.; Nickel, B.; Toccoli, T.; Chang, K.-C.; Mayer, A. C.; Clancy, P.; Blakely, J. M.; Headrick, R. L.; Iannotta, S.; Malliaras, G. G. Pentacene thin film growth. *Chem. Mater.* **2004**, *16*, 4497−4508.

(16) Lee, J. Y.; Roth, S.; Park, Y. W. Anisotropic Field Effect Mobility in Single Crystal Pentacene. *Appl. Phys. Lett.* **2006**, *88*, 252106.
(17) Lang, D. V.; Chi, X.; Siegrist, T.; Sergent, A. M.; Ramirez, A. P. Amorphous-like Density of Gap States in Single-Crystal Pentacene. *Phys. Rev. Lett.* **2004**, *93*, No. 086802.
(18) Haddon, R. C.; Chi, X.; Itkis, M. E.; Anthony, J. E.; Eaton, D. L.; Siegrist, T.; Mattheus, C. C.; Palstra, T. T. M. Band Electronic Structure of One- and Two-Dimensional Pentacene Molecular Crystals. *J. Phys. Chem. B.* **2002**, *106*, 8288−8292.
(19) Takeya, J.; Goldmann, C.; Haas, S.; Pernstich, K. P.; Ketterer, B.; Batlogg, B. Field-Induced Charge Transport at the Surface of Pentacene Single Crystals: A Method to Study Charge Dynamics of Two-Dimensional Electron Systems in Organic Crystals. *J. Appl. Phys.* **2003**, *94*, 5800−5804.
(20) Yang, H.; Yang, C.; Kim, S. H.; Jang, M.; Park, C. E. Dependence of Pentacene Crystal Growth on Dielectric Roughness for Fabrication of Flexible Field-Effect Transistors. *ACS Appl. Mater. Interfaces* **2010**, *2*, 391−396.
(21) Lee, H. S.; Kim, D. H.; Cho, J. H.; Hwang, M.; Jang, Y.; Cho, K. Effect of the Phase States of Self-Assembled Monolayers on Pentacene Growth and Thin-Film Transistor Characteristics. *J. Am. Chem. Soc.* **2008**, *130*, 10556−10564.
(22) Jurchescu, O. D.; Baas, J.; Palstra, T. T. M. Effect of Impurities on the Mobility of Single Crystal Pentacene. *Appl. Phys. Lett.* **2004**, *84*, 3061−3063.
(23) Kiguchi, M.; Nakayama, M.; Fujiwara, K.; Ueno, K.; Shimada, T.; Saiki, K. Accumulation and Depletion Layer Thicknesses in Organic Field Effect Transistors. *Jpn. J. Appl. Phys.* **2003**, *42*, L1408−L1410.
(24) Guo, D.; Miyadera, T.; Ikeda, S.; Shimada, T.; Saiki, K. Analysis of Charge Transport in a Polycrystalline Pentacene Thin Film Transistor by Temperature and Gate Bias Dependent Mobility and Conductance. *J. Appl. Phys.* **2007**, *102*, No. 023706.
(25) Ohtomo, M.; Suzuki, T.; Shimada, T.; Hasegawa, T. Band Dispersion of Quasi-Single Crystal Thin Film Phase Pentacene Monolayer Studied by Angle-Resolved Photoelectron Spectroscopy. *Appl. Phys. Lett.* **2009**, *95*, 123308.
(26) Shimada, T.; Nogawa, H.; Hasegawa, T.; Okada, R.; Ichikawa, H.; Ueno, K.; Saiki, K. Bulk-like pentacene epitaxial films on hydrogen-terminated Si(111). *Appl. Phys. Lett.* **2005**, *87*, No. 061917.
(27) Fukagawa, H.; Yamane, H.; Kataoka, T.; Kera, S.; Nakamura, M.; Kudo, K.; Ueno, N. Origin of the highest occupied band position in pentacene films from ultraviolet photoelectron spectroscopy: Hole stabilization versus band dispersion. *Phys. Rev. B* **2006**, *73*, No. 245310.
(28) Matsubara, R.; Ohashi, N.; Sakai, M.; Kudo, K.; Nakamura, M. Analysis of barrier height at crystalline domain boundary and in-domain mobility in pentacene polycrystalline films on SiO_2. *Appl. Phys. Lett.* **2008**, *92*, 242108.
(29) Sakai, N.; Tamura, T.; Yanase, T.; Nagahama, T.; Shimada, T. Single Crystal Growth, Structural Analysis and Electronic Band Structure of a Nitrogen-Containing Polyacene Benzo[i]benzo[6′,7′] quinoxalino [2′,3′:9,10] phenanthrol [4,5-abc] phenazine. *Jpn. J. Appl. Phys.* **2019**, *58*, SBBG08.
(30) Yanase, T.; Tanoguchi, H.; Sakai, N.; Jin, M.; Yamane, I.; Kato, M.; Ito, H.; Nagahama, T.; Shimada, T. Single Crystal Growth of π-Conjugated Large Molecules without Solubilizing Alkyl Chains via Naphthalene Flux Method. *Crystal Growth Des.* **2021**, *21*, 4683−4689.
(31) Laudise, R. A.; Kloc, C.; Simpkins, P. G.; Siegrist, T. Physical Vapor Growth of Organic Semiconductors. *J. Cryst. Growth* **1998**, *187*, 449−454.
(32) Arabi, S.; Atika, D. J.; Mirza, M.; Yu, P.; Wang, L.; He, J.; Jiang, C. Nanoseed Assisted PVT Growth of Ultrathin 2D Pentacene Molecular Crystal Directly onto SiO_2 Substrate. *Cryst. Growth Des.* **2016**, *16*, 2624−2630.
(33) Jin, Q.; Li, D.; Qi, Q.; Zhang, Y.; He, J.; Jiang, C. Two-Step Growth of Large Pentacene Single Crystals Based on Crystallization of Pentacene Monolayer Film. *Cryst. Growth Des.* **2012**, *12*, 5432−5438.
(34) Abe, T.; Matsubara, R.; Hayakawa, M.; Shimoyama, A.; Tanaka, T.; Tsuji, A.; Takahashi, Y.; Kubono, A. Measurement of incident molecular temperature in the formation of organic thin films. *Jpn. J. Appl. Phys.* **2018**, *57*, No. 03EG13.
(35) Maliakal, A.; Raghavachari, K.; Katz, H.; Chandross, E.; Siegrist, T. Photochemical Stability of Pentacene and a Substituted Pentacene in Solution and in Thin Films. *Chem. Mater.* **2004**, *16*, 4980−4986.
(36) Li, Y.; Wu, Y.; Liu, P.; Prostran, Z.; Gardner, S.; Ong, B. S. Stable Solution-Processed High-Mobility Substituted Pentacene Semiconductors. *Chem. Mater.* **2007**, *19*, 418−423.
(37) Sato, K.; Sawaguchi, T.; Sakata, M.; Itaya, K. Noncontact Atomic Force Microscopy of Perfect Single Crystals of Pentacene Prepared by Crystallization from Solution. *Langmuir* **2007**, *23*, 12788−12790.
(38) Kimura, Y.; Niwano, M.; Ikuma, N.; Goushi, K.; Itaya, K. Organic Field Effect Transistor Using Pentacene Single Crystals Grown by a Liquid-Phase Crystallization Process. *Langmuir* **2009**, *25*, 4861−4863.
(39) Ahn, I.-S.; Ghiorse, W. C.; Lion, L. W.; Shuler, M. L. Growth kinetics of Pseudomonas putida G7 on naphthalene and occurrence of naphthalene toxicity during nutrient deprivation. *Biotechnol. Bioeng.* **1998**, *59*, 587−594.
(40) Menezes, H. C.; Paulo, B. P.; Costa, N. T.; Cardeal, Z. L. New Method to Determination of Naphthalene in Ambient Air Using Cold Fiber-Solid Phase Microextraction and Gas Chromatography-Mass Spectrometry. *Microchem. J.* **2013**, *109*, 93−97.
(41) Siegrist, T.; Besnard, C.; Haas, S.; Schiltz, M.; Pattison, P.; Chernyshov, D.; Batlogg, B.; Kloc, C. A Polymorph Lost and Found: The High-Temperature Crystal Structure of Pentacene. *Adv. Mater.* **2007**, *19*, 2079−2082.
(42) Campbell, R. B.; Robertson, J. M.; Trotter, J. The Crystal and Molecular Structure of Pentacene. *Acta. Cryst.* **1961**, *14*, 705.
(43) Schiefer, S.; Huth, M.; Dobrinevski, A.; Nickel, B. Determination of the Crystal Structure of Substrate-Induced Pentacene Polymorphs in Fiber Structured Thin Films. *J. Am. Chem. Soc.* **2007**, *129*, 10316−10317.
(44) Mattheus, C. C.; Dros, A. B.; Baas, J.; Oostergetel, G. T.; Meetsma, A.; de Boer, J. L.; Palstra, T. T. M. Identification of polymorphs of pentacene. *Synth. Met.* **2003**, *138*, 475−481.
(45) Siegrist, T.; Kloc, C.; Schön, J. H.; Batlogg, B.; Haddon, R. C.; Berg, S.; Thomas, G. A. Enhanced Physical Properties in a Pentacene Polymorph. *Angew. Chem., Int. Ed.* **2001**, *40*, 1732−1736.
(46) Holmes, D.; Kumaraswamy, S.; Matzger, A. J.; Vollhardt, K. P. C. On the Nature of Nonplanarity in the [N]Phenylenes. *Chem. Europ. J.* **1999**, *5*, 3399−3412.
(47) Troisi, A.; Orlandi, G. Band Structure of the Four Pentacene Polymorphs and Effect on the Hole Mobility at Low Temperature. *J. Phys. Chem. B.* **2005**, *109*, 1849−1856.
(48) Momma, K.; Izumi, F. VESTA 3 for three-dimensional visualization of crystal, volumetric and morphology data. *J. Appl. Crystallogr.* **2011**, *44*, 1272−1276.
(49) Guo, D.; Sakamoto, K.; Miki, K.; Ikeda, S.; Saiki, K. Alignment-Induced Epitaxial Transition in Organic-Organic Heteroepitaxy. *Phys. Rev. Lett.* **2008**, *101*, No. 236103.

https://doi.org/10.1021/acsomega.2c03551
ACS Omega 2022, 7, 28618−28623